Available online at www.sciencedirect.com

SCIENCE DIRECT®

International Journal of Mass Spectrometry 233 (2004) 223–231

International Journal of Mass Spectrometry

www.elsevier.com/locate/ijms

Relative proton affinities from kinetic energy release distributions for dissociation of proton-bound dimers
2. Diamines as a test case[☆]

John J. Hache, Jean H. Futrell, Julia Laskin[*]

Pacific Northwest National Laboratory, Fundamental Science Directorate, P.O. Box 999 (K8-88), Richland, WA 99352, USA

Received 20 October 2003; accepted 21 December 2003

We are honored to have been asked and are pleased to dedicate this paper to Tilmann on the occasion of his sixtieth birthday.
We wish him every success in his ongoing highly successful career.

Abstract

Dissociation of proton-bound dimers containing diamines is often characterized by a substantial entropy difference between the two competing reaction channels. Kinetic energy release distributions (KERDs) upon dissociation of diamine-containing dimers are utilized along with Finite Heat Bath theory analysis to obtain relative proton affinities of monomeric species composing the dimer. When dissociation of a proton-bound dimer is not associated with reverse activation barrier our method provides reliable relative energetics and dynamics. Results are reported for 1,3-propanediamine–diisopropylamine, and 1,4-butanediamine–triethylamine dimers, for which the dynamics approach provided accurate values of relative proton affinities and relative reaction entropies. We also show two examples, for which a substantial reverse activation barrier is found using KER measurements. These examples point to potential problems with utilizing aromatic reference bases in combination with bidentate molecules for thermochemical determinations using the kinetic method.

Keywords: Kinetic energy release distribution (KERD); Dynamics approach; Proton-bound dimer; Dissociation; Diamine; Kinetic method; Relative energies; Reaction entropy

---

1. Introduction

Studies of competitive dissociation of proton-bound heterodimers via reactions 1 and 2 comprise the kinetic method—one of the most popular methods for thermochemical determinations in mass spectrometry [1,2].

$$[B_1-H^+\text{--}B_2]\begin{array}{ll} \xrightarrow{k_1} B_2 + B_1H^+ & (1) \\ \xrightarrow{k_2} B_2H^+ + B_1 & (2) \end{array}$$

The relative abundance of ionic fragments formed via reactions 1 and 2 is determined by their relative gas phase basicity. The branching ratio of the two reaction products is given by the following expression:

$$\ln\left(\frac{B_1H^+}{B_2H^+}\right) \cong \ln\left(\frac{k_1}{k_2}\right) = \frac{PA(B_1) - PA(B_2)}{RT_{eff}} - \frac{\Delta(S^{\ddagger})}{R} \quad (3)$$

where $\Delta(\Delta S^{\ddagger}) = \Delta S_2^{\ddagger} - \Delta S_1^{\ddagger}$ corresponds to the difference in entropies of activation in reactions 1 and 2; PA(B_1) and PA(B_2) are proton affinities of monomeric species B_1 and B_2, respectively; and T_{eff} is the effective temperature. It is commonly assumed that $\Delta(\Delta S^{\ddagger})$ can be closely approximated by the difference in protonation entropies of B_1 and B_2, i.e., $\Delta(\Delta S^{\ddagger}) \cong \Delta(\Delta S_p) = \Delta S_p(B_2) - \Delta S_p(B_1)$.

In the kinetic method branching ratios of reaction products are examined as a function of the proton affinity of the reference base, B_2. The kinetic plot is obtained by plotting $\ln(k_1/k_2)$ versus PA(B_2) [2]. According to Eq. (3) the

---

[☆] Two authors of this paper (J.L. and J.H.F.) have had the privilege of working with Professor Tilmann Märk as a colleague and coworker for several years—one of us (J.H.F.) for 25 years, beginning as a Fulbright Senior Scholar at the University of Innsbruck and continuing with greater or lesser intensity ever since. Professional visits to Innsbruck are always exciting because the Institut fuer Ionenphysik and Tilmann's group have become a focal point for fundamental studies of ion physics for scientists from many nations.

[*] Corresponding author. Tel.: +1-509-376-4443; fax: +1-509-376-3650.
E-mail address: Julia.Laskin@pnl.gov (J. Laskin).

1387-3806/$ – see front matter © 2004 Elsevier B.V. All rights reserved.
doi:10.1016/j.ijms.2003.12.022

slope of such a plot equals ($-1/RT_{\mathrm{eff}}$) and therefore determines the effective temperature, while the intercept equals $\mathrm{PA(B_1)}/RT_{\mathrm{eff}} - \Delta(\Delta S^{\ddagger})/R$. It follows that $\mathrm{PA(B_1)}$ can be determined from a single kinetic plot if the entropy difference for the two reaction channels is negligible. Alternatively, the entropic term can be separated by carrying out experiments at several effective temperatures using a set of structurally similar reference bases to ensure that $\Delta(\Delta S^{\ddagger})$ is the same for all reactions [3]. This can be done using collision-induced dissociation (CID) of dimers at different collision energies. A second plot of intercepts of the kinetic plots versus $1/RT_{\mathrm{eff}}$ enables determination of the proton affinity of the unknown from the slope and entropy difference from the intercept. The experimental entropy difference extracted from kinetic plots is commonly denoted as the apparent entropy difference, $\Delta\Delta S_{\mathrm{app}}$, to recognize that internal energy distribution of dissociating dimers is not necessarily close to thermal distribution at any temperature.

Basic assumptions of the kinetic method have been a subject of continuing debate in the literature [4–9]. In particular, the meaning of the effective temperature has been extensively discussed. Holmes and co-workers suggested that the ensemble of ions undergoing competing dissociation should be characterized by two different temperatures rather than by a single “effective” temperature. Indeed, our analysis of the kinetic method formalism using Finite Heat Bath Theory (FHBT) [10,11] demonstrated that the reacting population is described by two different transition state temperatures [9]. However, the effective temperature can be closely approximated by the transition state temperature for reaction 2. This finding justifies the use of the effective temperature.

Kinetic energy release distributions (KERDs) provide valuable information on the energetics and dynamics of unimolecular fragmentation in the gas phase. In the last decade many groups have contributed to this topic [12–19]. A comprehensive literature survey and a detailed discussion of various experimental and theoretical approaches for extracting thermochemical information from KERDs have been presented in a recent review [20]. The simplest theoretical approach based on FHBT developed by Klots [10,11] has been extensively utilized to quantify dissociation of cluster ions [13,14,18,19]. In particular, these studies focused on extracting dissociation energies for clusters of different composition and size from KERDs.

We have proposed a similar approach to obtain relative proton affinities of monomeric species composing proton-bound dimers using KERD measurements for two competing reaction channels 1 and 2 [9]. We refer to this method as the dynamics approach because KERD measurements are very sensitive to details of the potential energy surface for separating fragments. However, relative energetics for reactions with no reverse activation barrier can be obtained using this approach only if the excess internal energy is statistically partitioned into fragment ions. We start by defining three temperatures (see Fig. 1)—the temperature of the transition state for each reaction channel, $T_1^{\ddagger}$ and $T_2^{\ddagger}$, and the temperature of the excited ion, T. The latter reflects the internal energy of the activated proton-bound dimer, E, while transition state temperatures reflect the excess internal energy above the reaction threshold for reactions 1 and 2, namely, $E - \Delta E_1$ and $E - \Delta E_2$. FHBT is used to connect between $T^{\ddagger}$ and T and to calculate differences between dissociation energies and reaction entropies using the following procedure.

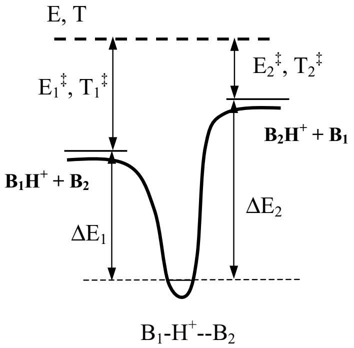

Fig. 1. Hypothetical potential energy surface for dissociation of a proton-bound dimer.

Specifically, KERDs for reactions with no reverse activation barrier can be presented in the following form [21]:

$$P(\varepsilon) = \varepsilon^{l} \exp\left(-\frac{\varepsilon}{k_{\mathrm{B}}T^{\ddagger}}\right) \tag{4}$$

where ε is the kinetic energy of the fragment in the center-of-mass (CM) frame, $P(\varepsilon)$ is the probability of finding fragment ion with a specific CM kinetic energy, l is a parameter ($0 < l < 1$); $T^{\ddagger}$ is the transition state temperature for reaction; k_{B} is Boltzmann’s constant. Fitting the experimental KERD with the above function yields the transition state temperature for the reaction. It follows that the two transition state temperatures, $T_1^{\ddagger}$ and $T_2^{\ddagger}$, can be determined by modeling KERDs for reactions 1 and 2. The difference in threshold energies for reactions 1 and 2 is given by:

$$\Delta E_2 - \Delta E_1 = \bar{E}_1^{\ddagger}(T_1^{\ddagger}) - \bar{E}_2^{\ddagger}(T_2^{\ddagger}) \tag{5}$$

where $\bar{E}^{\ddagger}(T^{\ddagger})$ is the average energy of the transition state evaluated at temperature $T^{\ddagger}$. If reactions 1 and 2 have negligible reverse activation barrier the relative proton affinity is then obtained from Eq. (6):

$$\mathrm{PA(B_1)} - \mathrm{PA(B_2)} = \Delta H_2 - \Delta H_1 = \Delta E_2 - \Delta E_1 \tag{6}$$

The difference in reaction entropies can be obtained from the measured branching ratio of the reaction products using Eq. (7) [9]:

$$\ln\left(\frac{k_1}{k_2}\right) = \frac{\Delta(\Delta S^{\ddagger})}{k_{\mathrm{B}}} + C \ln\left(\frac{T_1^{\ddagger}}{T_2^{\ddagger}}\right) \tag{7}$$

where C is the heat capacity of the energized ion at the temperature of the activated proton-bound dimer, T.

Recently we presented a study of dissociation of alcohol dimers and ethylenediamine–pyrrolidine dimer as a test case for the approach described above and demonstrated that it enables accurate measurement of relative proton affinities for a compound with unknown thermochemical properties versus a single reference base [22]. It also allows distinguishing cases when dissociation of proton-bound dimers is associated with a reverse activation barrier, for which both our approach and the kinetic method are inapplicable.

Dissociation of proton-bound dimers containing bases that di-coordinate the proton has been used to challenge the kinetic method. Protonation of bidentate molecules is characterized by a very large entropy effect because of proton solvation by the two basic sites of the molecule. Small diamines have been used by many groups [3,22–26] as model systems to determine the applicability of the kinetic method for determination of proton affinities of bidentate molecules. Siu and co-workers demonstrated that the kinetic method provides accurate PAs for small diamines [24], while other groups [23,25,26] suggested that PAs of diamines are underestimated by the kinetic method because of the presence of reverse activation barrier for dissociation. The latter was estimated by Cao et al. to be approximately 20 kJ/mol for 1,3-propanediamine and approximately 32 kJ/mol for 1,4-butanediamine [23]. Interestingly, no indication of the reverse activation barrier was obtained from kinetic energy release (KER) measurements [23]. The authors rationalized this discrepancy assuming that only a negligibly small fraction of the reverse activation energy was partitioned into relative translation of products.

In this work we present new results on KERD measurements for proton-bound dimers containing small diamines demonstrating both success and failure of the dynamics approach described above. We also identify potential difficulties associated with choice of reference bases for determination of proton affinities of bidentate molecules.

2. Experimental

Experiments were performed on a triple sector (EBE) Micromass ZabSpec (ZS017) mass spectrometer modified for accurate measurement of KERDs as described previously [22]. Mass-analyzed ion kinetic energy spectra (MIKEs) were obtained by scanning the second electric sector. Experimental metastable peaks were smoothed using a piecewise cubic spline smoothing routine. KERDs were obtained by differentiating the smoothed metastable peaks and converting the kinetic energy from the laboratory into the center-of-mass frame using a standard expression [20]. The values of KER reported in this work were obtained from the full widths of metastable peaks at 22% maximum and correspond to the average center-of-mass (CM) kinetic energy released into the relative translation of fragments.

Proton-bound dimers were generated in a CI source by self-protonation. The ion source conditions were as follows: source temperature, 100 °C; filament emission current, 0.6–1.1 mA; electron energy, 20–50 eV; pressure, 4×10^{-5} to 6×10^{-5} Torr, as monitored by the ionization gauge; acceleration voltage, 6 kV. The temperature of the liquid inlet system was optimized for the efficient formation of proton-bound dimers. All chemicals were purchased from Aldrich and used as received.

3. Modeling KERDs

3.1. Extracting transition state temperatures

Experimental metastable peaks were smoothed using a piecewise cubic spline smoothing routine. KERDs were obtained by differentiating the smoothed metastable peaks and converting the kinetic energy from the laboratory into the center-of-mass frame using a standard expression [20]. Experimental KERDs were fitted with the two-parameter function given in Eq. (4) to yield transition state temperatures for reactions 1 and 2. An example of a fit obtained for dissociation of the 1,3-propanediamine–diisopropylamine dimer is shown in Fig. 2.

3.2. Relative entropies

The difference in reaction entropies, $\Delta(\Delta S^{\ddagger})$, was calculated from the experimental branching ratio and the two transition state temperatures using Eq. (7). The dimensionless heat capacity was calculated using Eq. (8).

$$C = \sum_{i=1}^{N} \frac{(hc\nu_i/k_{\mathrm{B}}T)^2 \exp(-hc\nu_i/k_{\mathrm{B}}T)}{[1-\exp(-hc\nu_i/k_{\mathrm{B}}T)]^2} \qquad (8)$$

where ν_i are the vibrational frequencies, h is Planck's constant, k_{B} is Boltzmann's constant, T is the temperature, and c is the velocity of light. Vibrational frequencies for the 1,2-ethylenediamine–pyrrolidine dimer were adopted from our previous work [22]. The vibrational frequencies for protonated 1,3-propanediamine and 1,4-butanediamine were provided by Chris Rodriquez and Michael Siu (private communication). Vibrational frequencies for neutral triethylamine were estimated using AM1 calculations. The same set of frequencies was used for neutral diisopropylamine. Common modes of protonated dimers in the range 100–300 cm^{-1} were added to the combined frequency sets of the corresponding protonated and neutral species. Calculated results were not very sensitive to the values of vibrational frequencies. The uncertainties in the values of $\Delta(\Delta S^{\ddagger})$ and $\Delta(\Delta E)$ related to the uncertainties in vibrational frequencies are much smaller than the experimental error bars that have been assigned to the dissociation energy and entropy differences.

The heat capacity in Eq. (7) should be estimated at the temperature of the activated complex, T, which was deter-

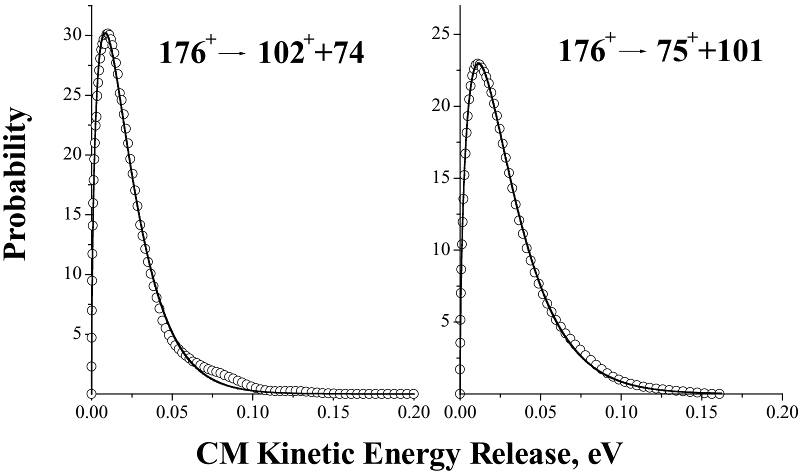

Fig. 2. Experimental (open circles) and calculated (solid line) KERDs for dissociation of the 1,3-propanediamine–diisopropylamine dimer ($m/z = 176$); left panel shows KERD extracted from the peak at $m/z = 102$ (protonated diisopropylamine), right panel shows KERD extracted from the peak at $m/z = 75$ (protonated 1,3-propanediamine).

mined via reiterative calculations to solve simultaneous Eqs. (8) and (9):

$$\frac{T}{T - T^{\ddagger}} \cong \frac{C}{\gamma}\left(1 + \frac{\gamma}{2C} + \frac{\gamma^2}{12C^2}\right) \qquad (9)$$

which represents the expression for the Carnot–Kelvin factor [21] with $\gamma = 23.5$—the Gspann parameter [21,27]. The average temperature of the transition states for reactions 1 and 2 was used to estimate the left hand side of Eq. (9). The uncertainty in the heat capacity associated with uncertainty in the value of the Gspann parameter is less than 10% and was taken into account when estimating the uncertainty in the relative entropy for reactions 1 and 2. Energy and entropy differences obtained in simulations utilizing individual transition state temperatures rather than the average value of $T^{\ddagger}$ in Eq. (9) are within the estimated uncertainties shown in Table 2.

3.3. Relative energies

The difference in the dissociation thresholds was obtained using Eq. (5). The average energy was calculated using a standard expression:

$$\langle E\rangle = \sum_{i=1}^{N} \frac{hc\nu_i}{\exp(hc\nu_i/k_{\mathrm{B}}T) - 1} \qquad (10)$$

Average energies of the two transition states (Eq. (5)) were calculated using transition state temperatures $T_1^{\ddagger}$ and $T_2^{\ddagger}$. It should be noted that $\bar{E}_1^{\ddagger}(T_1^{\ddagger})$ and $\bar{E}_2^{\ddagger}(T_2^{\ddagger})$ should be calculated using vibrational frequencies of the corresponding transition states for reactions 1 and 2. When entropy difference between the two reaction channels is small, the same set of frequencies can be used for calculating average energies. However, for dissociation of dimers containing diamines the entropy difference for reactions 1 and 2 is large. Consequently, vibrational frequencies for the two transition states become quite different and the difference between the average energies of the transition states may become quite sensitive to the entropy effect [28,29]. In order to account for these differences we generated a second set of transition state frequencies, in which 10 frequencies in the range 1000–1500 cm^{-1} were varied until the resulting entropy difference between the two sets of frequencies calculated using Eqs. (11) and (12) matched the entropy difference calculated using Eq. (7).

$$\Delta(\Delta S^{\ddagger}) \equiv \Delta S_2^{\ddagger} - \Delta S_1^{\ddagger} = R\left(\ln\frac{Q_2^{\ddagger}}{Q_1^{\ddagger}} + T\frac{\mathrm{dln}(Q_2^{\ddagger}/Q_1^{\ddagger})}{\mathrm{d}T}\right) \qquad (11)$$

where $Q^{\ddagger}$ is the partition function of the transition state:

$$Q^{\ddagger} = \sum_{i=1}^{N} \frac{1}{1 - \exp(-hc\nu_i/k_{\mathrm{B}}T)} \qquad (12)$$

The entropy difference in Eq. (11) was calculated at the temperature of the excited dimer, T.

4. Results and discussion

Metastable peak shapes and branching ratios were measured for dissociation of the following proton-bound dimers: 1,2-ethylenediamine–3-Piccoline, 1,2-ethylenediamine–4-Piccoline, 1,3-propanediamine–diisopropylamine, and 1,4-butanediamine–triethylamine. The results for 1,2-ethylenediamine–pyrrolidine dimer were adopted from our previous work [22] for comparison.

4.1. Kinetic energy releases (KERs) and branching ratios

Table 1 lists gas phase basicities and proton affinities for all monomers obtained from NIST database [30] along

Table 1
Proton affinities, average kinetic energy releases and branching ratios for proton-bound dimers of different diamines

	GB (kcal/mol)[a]	PA (kcal/mol)[a]	KER (meV)	BR[b]
Ethylenediamine (B_1)	218.1	227.4	32	0.085
Pyrrolidine (B_2)	218.8	226.6	26	
Ethylenediamine (B_1)	218.1	227.4	81	1.11
3-Piccoline (B_2)	217.9	225.5	28	
Ethylenediamine (B_1)	218.1	227.4	83	0.152
4-Piccoline (B_2)	218.8	226.4	28	
Propanediamine (B_1)	224.7	235.9	32	1.95
Diisopropylamine (B_2)	224.3	232.3	24	
Butanediamine (B_1)	228.1	240.3	30	41
Triethylamine (B_2)	227.0	234.7	24	

[a] Gas phase basicities and proton affinities of monomers from Ref. [30].
[b] Branching ratio, B_1H^+/B_2H^+.

with experimentally determined KERs and branching ratios for dissociation of proton-bound dimers. The branching ratios clearly indicate preferential formation of a monomer with higher gas phase basicity during fragmentation of a proton-bound dimer.

Kinetic energy releases also show a clear trend: higher proton affinity is associated with larger KER. For example, for ethylenediamine–pyrrolidine dimer larger KER (32 meV) was observed for the monomer with larger proton affinity (227.4 kcal/mol), while smaller KER (26 meV) is observed for protonated pyrrolidine (PA = 226.6 kcal/mol). This observation can be rationalized using a hypothetical potential energy surface for dissociation of a dimer with internal energy E shown in Fig. 1. If the proton affinity of B_1 is higher than the proton affinity of the reference base, the threshold energy for reaction 1 (ΔE_1) is lower than the threshold energy for reaction 2 (ΔE_2). Consequently, reaction 1 is characterized by higher excess internal energy ($E_1^{\ddagger}$), higher transition state temperature ($T_1^{\ddagger}$), and larger KER; i.e., the higher proton affinity is associated with larger experimental KER.

4.2. Dissociation of dimers containing 1,2-ethylenediamine

Formation of protonated 1,2-ethylenediamine was examined using three reference bases shown in Scheme 1. Results shown in Table 1 indicate that formation of protonated 1,2-ethylenediamine is associated with anomalously large KER when 3-Picoline or 4-Picoline are used as reference bases—81 and 83 meV, respectively. This should be compared to only 32 meV obtained when pyrrolidine was used as a reference base. KER data summarized in Table 1 indicate the presence of the reverse activation barrier for formation of protonated 1,2-ethylenediamine from dimers containing 3-Picoline and 4-Picoline. The position, shape and width of KERD for reactions with reverse activation barrier depends on the steepness of the potential energy surface beyond the transition state and the degree of coupling of various vibrational modes during separation of the ionic and neutral fragment. As shown in Fig. 3, the shape of KERDs extracted from the corresponding metastable peaks is very similar to KERDs obtained for other dissociation channels and is not shifted from zero. This indicates that the reverse activation energy is only partially released into the relative translation of the products. This results from coupling of the reaction coordinate with other vibrational modes in the dimer after the passage over the dissociation barrier [20]. The transition state temperatures extracted from these KERDs are close to 650 K. This implies a relative proton affinity of more than 25 kcal/mol, which is not a reasonable value. This confirms that neither the dynamics approach nor the kinetic method can be used for determination of relative proton affinities from characterizing the dissociation of 1,2-ethylenediamine–picoline dimers.

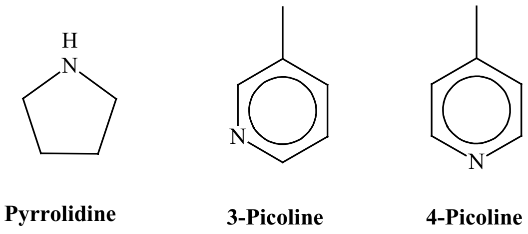

Scheme 1.

Our observation of the presence of a reverse activation barrier for dissociation of dimers containing 1,2-ethylenediamine and 3- or 4-Picoline suggests that formation of protonated 1,2-ethylenediamine from these dimers requires substantial rearrangement. In contrast, there is no reverse activation barrier for formation of protonated 3-Picoline and 4-Picoline bases from these dimers. These results indicate that in the transition state 1,2-ethylenediamine has to first open up and then re-close when it is leaving as a protonated species, while neutral 1,2-ethylenediamine does not undergo any additional rearrangement. We infer that in the protonated dimer of 1,2-ethylenediamine with picoline diamine interacts with the aromatic ring, while in the 1,2-ethylenediamine–pyrrolidine dimer the two monomers are coordinated to the nitrogen of the five-membered ring. In the former case 1,2-ethylenediamine most probably has an elongated structure while it is coordinated to the reference base. Theoretical calculation on the structure of 1,2-ethylenediamine–picoline dimers is presently underway in our laboratory to test this hypothesis.

Because of the reverse activation barrier fragmentation of 1,2-ethylenediamine–picoline dimers cannot be treated using the kinetic method. However, KERD measurements are usually not performed in the kinetic method studies. Without a prior knowledge of potential problems associated with the choice of reference bases for 1,2-ethylenediamine one could try to determine the relative proton affinity using branching ratios from Table 1. Fig. 4 shows a kinetic plot for dimers containing 1,2-ethylenediamine. Interestingly, a

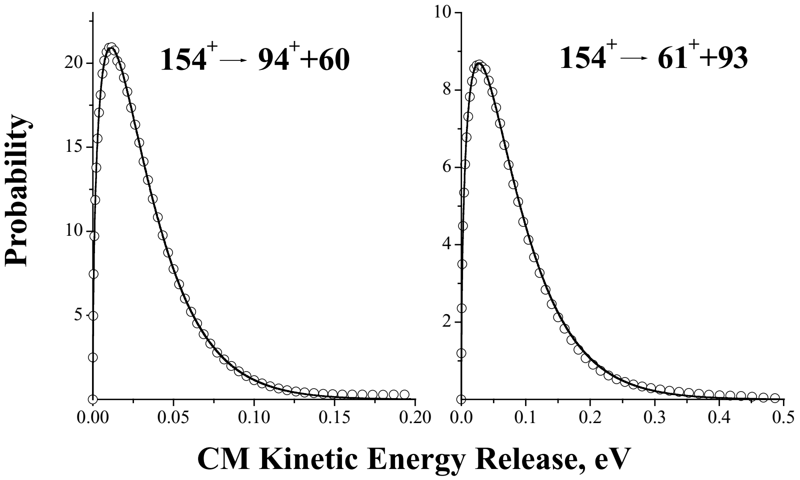

Fig. 3. Experimental (open circles) and calculated (solid line) KERDs for dissociation of the 1,2-ethylenediamine–3-Picoline dimer ($m/z = 154$); left panel shows KERD extracted from the peak at $m/z = 94$ (protonated 3-Picoline), right panel shows KERD extracted from the peak at $m/z = 61$ (protonated 1,2-ethylenediamine).

very good-quality plot is obtained for these systems. The effective temperature extracted from the slope of this plot is very close to the transition state temperatures obtained for 1,2-ethylenediamine–pyrrolidine dimer (see Table 2). However, only one data point on this plot (indicated by an arrow) can be used for kinetic measurements. These results demonstrate that because measurements of branching ratios are not sensitive to the presence of reverse activation barrier for reaction great care should be taken while choosing reference bases for kinetic measurements. In addition KER measurements are very important for validating the choice and applicability of reference bases for each particular case.

4.3. Dissociation of other diamine-containing dimers

According to Table 1 dissociation of 1,2-ethylenediamine–pyrrolidine, 1,3-propanediamine–diisopropylamine, and 1,4-butanediamine–triethylamine dimers is not associated with reverse activation barriers; i.e., these systems are good candidates for testing the dynamics approach. A sum-

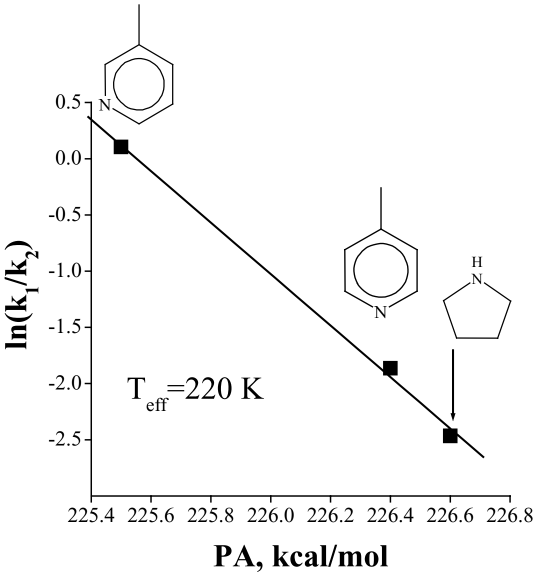

Fig. 4. Kinetic plot for dissociation of proton-bound dimers of 1,2-ethylenediamine with different bases.

Table 2
Transition state temperatures, relative dissociation energies and entropies obtained from KERDs

$B_1 \cdots H^+ \cdots B_2$	Br[a]	$T_1^{\ddagger}$ (K)	$T_2^{\ddagger}$ (K)	$\Delta E_1 - \Delta E_2$[b]	$PA_2 - PA_1$[c]	$\Delta(\Delta S^{\ddagger})$[d]	$\Delta(\Delta S_p)$[e]	$\bar{E}_1^{\ddagger}(T_1^{\ddagger})$ (eV)	$\bar{E}_2^{\ddagger}(T_2^{\ddagger})$ (eV)	$\Delta\Delta S_{app}$[f]
Ethylenediamine ($m/z = 61$)–pyrrolidine ($m/z = 72$)	0.085	212	200	−0.7 ± 0.3	−0.80	−8.3 ± 3.0	−5.0	0.116	0.086	−3.3
Propanediamine ($m/z = 75$)–diisopropylamine ($m/z = 102$)	1.95	230	190	−2.0 ± 0.7	−3.60	−12.0 ± 3.5	−10.7	0.177	0.093	−9.2
Butanediamine ($m/z = 89$)–triethylamine ($m/z = 102$)	41	265	190	−4.7 ± 1.0	−5.64	−18.3 ± 4.0	−15.1	0.308	0.104	−22.1

[a] Branching ratio, B_1H^+/B_2H^+.

[b] The difference in threshold energies for reactions 1 and 2 in kcal/mol.

[c] The difference in proton affinities of B_2 and B_1 in kcal/mol [30].

[d] The difference in reaction entropies for reactions 1 and 2 in cal/mol K.

[e] The difference in protonation entropies from Ref. [30] in cal/mol K.

[f] The apparent entropy difference calculated using Eq. (13).

Table 3
Energetic and entropic contributions to branching ratios

$B_1 \cdots H^+ \cdots B_2$	C[a]	T (K)[b]	$\ln(k_1/k_2)$	$C\ln(T_1^{\ddagger}/T_2^{\ddagger})$	$\Delta(\Delta S^{\ddagger})/R$[c]
Ethylenediamine ($m/z = 61$)–pyrrolidine ($m/z = 72$)	29.18	461	−2.47	1.70	−4.17
Propanediamine ($m/z = 75$)–diisopropylamine ($m/z = 102$)	34.97	411	0.67	6.68	−6.01
Butanediamine ($m/z = 89$)–triethylamine ($m/z = 102$)	38.81	417	3.71	12.91	−9.20

[a] Dimensionless heat capacity.
[b] The temperature of the activated complex.
[c] $\Delta\Delta S = \Delta S_1 - \Delta S_2$.

mary of relative energies and entropies obtained for these systems is given in Table 2. The relative energies obtained from KERD measurements are in excellent agreement with literature data. The absolute values of the relative reaction entropies are fairly close to but systematically larger than the differences in protonation entropies, $\Delta(\Delta S_p)$. This systematic deviation between the experimentally determined values of $\Delta(\Delta S^{\ddagger})$ and the differences in protonation entropies of monomeric species results from differences in temperatures. Specifically, $\Delta(\Delta S_p)$ are reported for 298 K, while the values of $\Delta(\Delta S^{\ddagger})$ correspond to temperatures in excess of 400 K (see Table 3). The corresponding entropy differences, $\Delta(\Delta S^{\ddagger})$, scaled to 298 K are −4.8, −7.3 and −12.6 cal/mol K for the ethylenediamine–pyrrolidine, propanediamine–diisopropylamine, and butanediamine–triethylamine, respectively. It follows that for dissociation of proton-bound dimers examined in this study the differences between the activation entropies determined using the dynamic approach and the relative protonation entropies are the same within the experimental uncertainty.

It should be noted that $\Delta(\Delta S^{\ddagger})$ derived from experimental data using Eq. (7) is very sensitive to transition state temperatures. This sensitivity is determined by the value of the heat capacity, C, that effectively amplifies the small differences in transition state temperatures. Small uncertainties in the transition state temperatures are translated into a large error in determination of the relative reaction entropy. However, this sensitivity to transition state temperatures should not be confused with the general temperature dependence of the reaction entropy, which is very slow. The uncertainties in $\Delta(\Delta S^{\ddagger})$ listed in Table 2 are typical for experimental determination of reaction entropies.

In our previous study we demonstrated good correspondence between the relative entropies obtained from kinetic plots and relative reaction entropies calculated using Eqs. (11) and (12) [9]. However, entropy differences examined in that study did not exceed 3 cal/mol K as compared to 5–20 cal/mol K derived in this study. Recently, Erwin presented a detailed simulation of kinetic method experiments using the phase space limit (PSL) calculations of microcanonical rate constants [31]. Apparent entropy factors derived from kinetic plots did not agree well with thermodynamic entropy differences calculated at several temperatures. Erwin concluded that the relative entropies extracted from kinetic plots do not reflect thermodynamic entropy differences but rather correspond to the ratio of the microcanonical sum of states for the two transition states evaluated at the mean internal energy of dissociating ions.

We have calculated the entropy differences using the approach suggested by Erwin. Namely, we used the following expression:

$$\Delta\Delta S_{\text{app}} = R\frac{W_2^{\ddagger}(\bar{E}_2^{\ddagger}(T_2^{\ddagger}))}{W_1^{\ddagger}(\bar{E}_1^{\ddagger}(T_1^{\ddagger}))} \qquad (13)$$

where $W_1^{\ddagger}(\bar{E}_1^{\ddagger}(T_1^{\ddagger}))$ and $W_2^{\ddagger}(\bar{E}_2^{\ddagger}(T_2^{\ddagger}))$ represent sums of states of the two transition states at the corresponding average energy determined from KERDs as described earlier and R is the molar gas constant. Sums of states were calculated using Beyer-Swinehart direct count algorithm [32]. The results of these calculations are shown in Table 2. Because of the uncertainties in the transition state temperatures $\Delta\Delta S_{\text{app}}$ have similar error bars to $\Delta(\Delta S^{\ddagger})$. It can be seen that there is reasonable correspondence between the calculated values of $\Delta\Delta S_{\text{app}}$ and $\Delta(\Delta S_p)$. However, unlike the values of $\Delta(\Delta S^{\ddagger})$ that are systematically larger than $\Delta(\Delta S_p)$, apparent entropy differences determined using Eq. (13) show both positive and negative deviation from $\Delta(\Delta S_p)$. These deviations mainly result from uncertainties in transition state temperatures and are particularly important when the average energy of the transition state is small.

Good correspondence between entropy terms obtained using Eqs. (7) and (13) is not surprising. Although the internal energy distribution of the ensemble of ions that undergoes fragmentation in a mass spectrometer is not close to Boltzmann distribution, evaluation of the “microcanonical entropy” using the *average energy* of the fragmenting molecules equates the canonical and microcanonical approaches because it neglects differences in the shapes of internal energy distributions. We are unable to rationalize why Erwin’s calculations demonstrated a significant difference between the thermodynamic entropy and the entropy calculated using Eq. (13).

A final comment relates to experimental determination of entropy differences for reactions using the kinetic method. We have shown earlier that careful choice of reference bases is an important prerequisite for success of the kinetic method. This is particularly important for entropy measurements. In most cases differences in proton affinities between monomers composing the dimer do not exceed 5 kcal/mol, which sets a corresponding upper limit for error in determination of the proton affinity. In marked contrast, entropy differences between the two competing reactions can be very significant. Entropy differences can be obtained using the extended version of the kinetic method, in which dissociation of dimers is examined at different collision energies [3]. Dissociation of proton-bound dimers with some of the reference bases may be associated with a reverse activation barrier. If such bases are present in the set chosen for kinetic measurements, the behavior of the kinetic plot as a function of collision energy cannot be predicted on an a priori basis.

4.4. Factors that contribute to the branching ratio

It is interesting to examine the relative contribution of the energetics and dynamics of dissociation to the branching ratio of the reaction products. This can be done using Eq. (7), in which the first term on the right hand side, represents the entropy contribution, while the second term, $C\ln(T_1^{\ddagger}/T_2^{\ddagger})$, represents the contribution that originates from the differences in dissociation energies. Table 3 shows the values of the different terms in Eq. (7) along with the dimensionless heat capacities, C, and the temperatures of excited dimers, T. Clearly, when the transition state temperatures for the two reactions are similar (as for the 1,2-ethylenediamine–pyrrolidine dimer) the entropic term is dominant. However, because of a substantially larger difference in transition state temperatures the relative contribution of the entropy term decreases for dimers containing 1,3-propanediamine and 1,4-butanediamine. It should be noted that contribution of the heat capacity in the energy term, $C\ln(T_1^{\ddagger}/T_2^{\ddagger})$, to the branching ratio is expected to increase with increase in the size of the dimer. It should be noted that these findings are in a qualitative agreement with the standard kinetic method expression (Eq. (3)), which predicts a similar interplay between the entropy and the energy term. However, our approach provides a simple means of independent measurement of entropy and energy effects in competitive dissociation of dimers.

5. Conclusions

This work has extended our previous study on determination of relative proton affinities of monomers containing proton-bound dimers based on KERD measurements. The relative energetics of the two competing reactions is determined using transition state temperatures for each reaction channel extracted from the corresponding KERD. In contrast with the kinetic method approach proton affinity determination is not coupled to measurement of the branching ratio. However, the relative entropy for dissociation of the dimer into two charged monomers is determined by combining the branching ratio with the transition state temperatures. We have demonstrated that the entropy contribution to the branching ratio is dominant when the transition state temperatures are similar. However, for significantly different transition state temperatures the energetic term becomes quite large. Our results suggest that the relative contribution of the energetic term is expected to increase for larger dimers.

When dissociation of a proton-bound dimer is not associated with reverse activation barrier the dynamics approach provides reliable relative energetics and dynamics. The differences between the values of $\Delta(\Delta S^{\ddagger})$ determined from experimental data and the literature values of $\Delta(\Delta S_{\mathrm{p}})$ result from differences in temperatures used to evaluate these entropy terms. When properly scaled to 298 K the differences between the activation entropies determined using the dynamic approach and the relative protonation entropies are the same within the experimental uncertainty. Comparison between the thermodynamic entropy difference and the entropy difference obtained from the number of states in the transition state for each reaction channel demonstrates that both approaches provide similar values of relative entropies for competing reactions.

We have further demonstrated that careful choice of reference bases for the kinetic method studies is not a trivial task. KERs upon dissociation of 1,2-ethylenediamine with two aromatic molecules used as reference bases (3-Picoline and 4-Picoline) indicated the presence of the reverse activation barrier, while dissociation of the 1,2-ethylenediamine–pyrrolidine dimer did not show any rearrangement. We suggested that in the former case ethylenediamine has an elongated structure in the dimer and undergoes a substantial rearrangement following fragmentation of the dimer by closing the ring when it carries the proton. Despite the presence of the reverse activation barrier for dissociation of two of three ethylenediamine dimers examined in this study a good-quality kinetic plot was obtained for 1,2-ethylenediamine. This indicates that results obtained using branching ratios alone can be misleading. We conclude that KER measurements are very important to test the applicability of different reference bases for thermochemical determinations using the kinetic method.

Acknowledgements

All of the work described herein was conducted at the W.R. Wiley Environmental Molecular Sciences Laboratory (EMSL), a national scientific user facility sponsored by the U.S. Department of Energy and located at Pacific Northwest National Laboratory. PNNL is operated by Battelle for the U.S. Department of Energy. Research at EMSL was carried out within the project 40457 supported by the Office of Basic Energy Sciences of the U.S. Department of Energy. One of us (J.J.H.) was supported by ERULF fellowship, which is gratefully acknowledged. The authors are thankful to Chris Rodriquez and Michael Siu (York University, Toronto) for providing us with vibrational frequencies of protonated diamines. We would also like to thank Terry McMahon and Douglas Ridge for very helpful discussions.

References

[1] R.G. Cooks, T.L. Kruger, J. Am. Chem. Soc. 99 (1977) 1279.

[2] S.A. McLuckey, D. Cameron, R.G. Cooks, J. Am. Chem. Soc. 103 (1981) 1313.

[3] X. Cheng, Z. Wu, C. Fenselau, J. Am. Chem. Soc. 115 (1993) 4844.

[4] R.G. Cooks, J.T. Koskinen, P.D. Thomas, J. Mass Spectrom. 34 (1999) 85.

[5] P.B. Armentrout, J. Mass Spectrom. 34 (1999) 74.

[6] L. Drahos, K. Vékey, J. Mass Spectrom. 34 (1999) 79.

[7] J.L. Holmes, C. Aurby, P.M. Mayer, J. Phys. Chem. A 103 (1999) 705.

[8] J. Cao, J.L. Holmes, Int. J. Mass Spectrom. 195/196 (2000) 525.

[9] J. Laskin, J.H. Futrell, J. Phys. Chem. A 104 (2000) 8829.

[10] C.E. Klots, J. Chem. Phys. 90 (1989) 4470.

[11] C.E. Klots, in: C.Y. Ng, T. Baer, I. Powis (Eds.), Unimolecular and Bimolecular Reaction Dynamics, Wiley, 1994.

[12] (a) M.A. Hanratty, J.L. Beauchamp, A.J. Illies, P. van Koppen, M.T. Bowers, J. Am. Chem. Soc. 110 (1988) 1;
(b) P.A.M. van Koppen, D.B. Jacobson, A. Illies, M.T. Bowers, M. Hanratty, J.L. Beauchamp, J. Am. Chem. Soc. 111 (1989) 1991;
(c) P.A.M. van Koppen, J. Brodbelt-Lustig, M.T. Bowers, D.V. Dearden, J.L. Beauchamp, E.R. Fisher, P.B. Armentrout, J. Am. Chem. Soc. 112 (1990) 5663;
(d) P.A.M. van Koppen, J. Brodbelt-Lustig, M.T. Bowers, D.V. Dearden, J.L. Beauchamp, E.R. Fisher, P.B. Armentrout, J. Am. Chem. Soc. 113 (1991) 2359.

[13] (a) C.E. Klots, J. Chem. Phys. 98 (1993) 1110;
(b) C.E. Klots, J. Chem. Phys. 100 (1994) 1035.

[14] (a) C. Lifshitz, in: T. Baer, C.Y. Ng, I. Powis (Eds.), Current Topics in Ion Chemistry and Physics: Clusters, Wiley, New York, 1993, p. 122;
(b) C. Lifshitz, F. Louage, J. Phys. Chem. 93 (1989) 5633;
(c) C. Lifshitz, F. Louage, Int. J. Mass Spectrom. Ion Process. 101 (1990) 101.

[15] (a) J.C. Lorquet, B. Leyh, Org. Mass Spectrom. 28 (1993) 1225;
(b) P. Urbain, F. Remacle, B. Leyh, J.C. Lorquet, J. Phys. Chem. 100 (1996) 8003;
(c) P. Urbain, B. Leyh, F. Remacle, A.J. Lorquet, R. Flammang, J.C. Lorquet, J. Chem. Phys. 110 (1999) 2911;
(d) P. Urbain, B. Leyh, F. Remacle, J.C. Lorquet, Int. J. Mass Spectrom. 185–187 (1999) 155;
(e) A. Hoxha, R. Locht, J.C. Lorquet, B. Leyh, J. Chem. Phys. 111 (1999) 9259;
(f) J.C. Lorquet, Int. J. Mass Spectrom. 201 (2000) 59.

[16] (a) C.E. Klots, D. Mintz, T. Baer, J. Chem. Phys. 66 (1977) 5100;
(b) T. Baer, U. Buchler, C.E. Klots, J. Chim. Phys. 77 (1980) 739;
(c) W.A. Brand, T. Baer, C.E. Klots, Chem. Phys. 76 (1983) 111;
(d) B.E. Miller, T. Baer, Chem. Phys. 85 (1984) 39;
(e) D.M. Mintz, T. Baer, J. Chem. Phys. 65 (1976) 2407;
(f) T. Baer, T.E. Carney, J. Chem. Phys. 76 (1982) 1304.

[17] (a) J.C. Choe, M.S. Kim, Int. J. Mass Spectrom. Ion Process. 107 (1991) 103;
(b) D.Y. Kim, J.C. Choe, M.S. Kim, J. Chem. Phys. 113 (2000) 1714.

[18] (a) P. Sandler, T. Peres, G. Weissman, C. Lifshitz, Ber. Bunsenges Phys. Chem. 96 (1992) 1195;
(b) P. Sandler, C. Lifshitz, C.E. Klots, Chem. Phys. Lett. 200 (1992) 445;
(c) W.Y. Feng, C. Lifshitz, J. Phys. Chem. 98 (1994) 6075;
(d) J. Laskin, H.A. Jimenez-Vazquez, R. Shimshi, M. Saunders, M.S. de Vries, C. Lifshitz, Chem. Phys. Lett. 242 (1995) 249;
(e) J. Laskin, T. Peres, A. Khong, H.A. Jiménez-Vázquez, R.J. Cross, M. Saunders, D.S. Bethune, M.S. de Vries, C. Lifshitz, Int. J. Mass Spectrom. Ion Process. 187 (1999) 61.

[19] (a) S. Matt, O. Echt, M. Sonderegger, R. David, P. Scheier, J. Laskin, C. Lifshitz, T.D. Märk, Chem. Phys. Lett. 303 (1999) 379;
(b) R. Parajuli, S. Matt, O. Echt, A. Stamatovic, P. Scheier, T.D. Märk, Eur. Phys. J. D 16 (2001) 69;
(c) K. Gluch, J. Fedor, S. Matt-Leubner, R. Parajuli, C. Mair, A. Stamatovic, O. Echt, C. Lifshitz, J. Harvey, F. Hagelberg, Z. Herman, M. Probst, P. Scheier, T.D. Märk, Eur. Phys. J. D 24 (2003) 131.

[20] J. Laskin, C. Lifshitz, J. Mass Spectrom. 36 (2001) 459.

[21] C.E. Klots, Z. Phys. D 21 (1991) 335.

[22] J.J. Hache, J. Laskin, J.H. Futrell, J. Phys. Chem. A 106 (2002) 12051.

[23] J. Cao, C. Aubry, J.L. Holmes, J. Phys. Chem. A 104 (2000) 10045.

[24] Z. Wang, I.K. Chu, C.F. Rodriquez, A.C. Hopkinson, K.W.M. Siu, J. Phys. Chem. A 103 (1999) 8700.

[25] G. Bouchoux, F. Djazi, F. Gaillard, D. Vierezet, Int. J. Mass Spectrom. 227 (2003) 479.

[26] I.-S. Hahn, C. Wesdemiotis, Int. J. Mass Spectrom. 222 (2003) 465.

[27] C. Lifshitz, in: C.Y. Ng, T. Baer, I. Powis (Eds.), Cluster Ions, Wiley, 1993 (Chapter 2).

[28] J. Laskin, T.H. Bailey, E.V. Denisov, J.H. Futrell, J. Phys. Chem. A 106 (2002) 9832.

[29] J. Laskin, J.H. Futrell, J. Phys. Chem. A 107 (2003) 5836.

[30] P.J. Linstrom, W.G. Mallard (Eds.), NIST Chemistry WebBook, NIST Standard Reference Database Number 69, March 2003.

[31] K.M. Erwin, J. Am. Soc. Mass Spectrom. 13 (2002) 435.

[32] K.A. Holbrook, M.J. Pilling, S.H. Robertson, Unimolecular Reactions, Wiley, New York, 1996.